Assessing the Applicability of Sentinel-1 SAR Data for Semi-automatic Detection of Snow-avalanche Debris in the Southern Tyrolean Alps

GI_Forum 2023, Issue 2
Page: 59 - 68
Short Paper
Corresponding Author:
mattia19@hotmail.com
DOI: 10.1553/giscience2023_02_s59

Mattia Sartori[1] and Zahra Dabiri[1]
[1]Salzburg University, Austria

Abstract

Snow avalanches threaten the safety of people and infrastructure, causing casualties and damage every year. Essential information about spatial distribution and size of avalanches, for mitigation measures, hazard mapping and forecasting, is currently incomplete. Long-term avalanche monitoring over large regions can best be achieved using a space-borne synthetic aperture radar (SAR) system, which offers broad, all-weather coverage, day and night, ensuring data continuity. This study aims to assess the applicability of Sentinel-1 SAR data to semi-automatically detect avalanche debris in the western part of the Italian southern Tyrol, using the snow-rich period of January 2018 as a reference. Utilizing SAR data, avalanche debris was detected by identifying changes in backscatter caused by the rough snow in the avalanche's run-out zone. Change detection was performed by comparing post- and pre-event Sentinel-1 SAR images and unsupervised object-based classification. 79% of avalanches within the usable portions of the SAR images were correctly detected. Further investigation is required to assess the applicability of the proposed model on a regional scale.

Keywords:

Sentinel-1 SAR, unsupervised object classification, change detection, avalanche debris

1 Introduction

Between 2018 and 2022, snow avalanches caused the deaths of 347 people, with 129 casualties in the winter season 2020–2021 alone in Europe (EAWS, 2023). Especially in densely populated mountainous regions, these events can be extremely destructive, endangering people and infrastructure (Yang et al., 2020).

Forecasting, by predicting snow instability in space and time, is currently the most important measure to mitigate hazards and avoid exposure to avalanches (McClung, 2002). In the Alps, forecasting is implemented through a regional bulletin, issued daily during the winter months, which informs people about the current danger level (avalanche.report/bulletin/latest).

This forecasting system could be improved by integrating knowledge about past avalanche events. This could allow better understanding of the distribution and occurrence of avalanches over broader temporal and spatial scales, and the recognition of patterns and of zones with recurrent danger (Hafner et al., 2021), as well as hazard mapping and forecasting (Muller et al., 2021). The resulting database containing information about avalanche debris distribution over an entire winter season could deepen the knowledge of danger zones, thus creating a reliable base to improve safety for people and infrastructure in the mountains.

Target physical properties, such as surface roughness and dielectric properties, can affect SAR backscatter data (Kumar et al., 2022). Changes in backscatter values in SAR images taken before the avalanche happened (baseline images) and post-event can be used to distinguish between smooth and rough snow. Sentinel-1 SAR data can be used to detect only the run-out zone of an avalanche – that is, the bottom section where snow debris piles up and produces a rough surface that reflects radar waves differently from the surrounding undisturbed snow (Leinss et al., 2020).

Hazard mapping using multitemporal SAR images for avalanche detection is not new, but in its early stages it relied mainly on expert interpretation (Wiesmann et al., 2001). More recently, classification and segmentation algorithms have been developed to automatically identify avalanche debris. For example Wesselink et al. (2017) used an automatic detection algorithm based on backscatter thresholding, but the method has the drawback of marked over-detection. Vickers et al. (2017) used change detection and K-means classification, and applied improved filtering on images to obtain satisfactory detection results. Eckerstorfer et al. (2019) used a near-real-time detection system that achieves 79% accuracy in cases of medium to large avalanches. The system is already operational in some regions of Norway. Hafner et al. (2021) evaluate performance and completeness by comparing optical and radar imagery and confirm the reliability of Sentinel-1 SAR data for avalanche detection. Recent work has applied deep learning methods for avalanche detection in SAR images. Sinha et al. (2019), for example, used convolutional neural networks to locate avalanche debris signatures on SAR image patches. Bianchi et al. (2021) applied the same method but approached the segmentation task at the pixel level instead of the patch level, making the segmentation independent of the window size. While these methods are very promising, they rely on expert labelling, which brings limitations, including reliability, availability of an expert to train large datasets, and difficulties in differentiating between new avalanches and (still visible) old ones. Sinha et al. (2019) proposed deep unsupervised learning using a variational auto-encoder as a new benchmark in avalanche detection that outperforms previous methods. Although labelled data is required only in the validation phase, a form of training by an expert is still necessary.

This study aims to create a model to semi-automatically identify avalanche debris in the western part of the southern Tyrol using Sentinel-1 (C-band) SAR data and unsupervised object-based classification. The results were compared to reference maps from officially reported avalanches in order to assess their accuracy and reliability.

Avalanche detection can also be performed successfully using optical imagery, as in the automatic detection model based on SPOT 6/7 data using deep learning (Hafner et al., 2022). However, in order to ensure data continuity and broad coverage, we deliberately focused on the potential of SAR data, as the applicability of optical data is limited in areas with high cloud coverage. Furthermore, we aimed for maximum automation of the avalanche detection model, which made the choice of SAR data sensible.

2 Materials and Methods

The study area is located in the western part of the southern Tyrol, in the northern Italian Alps, close to the border with Austria (Figure 1). It covers approximately 2,000 km², comprising inhabited alpine valleys used for fruit tree cultivation and pastures, which are surrounded by peaks reaching 3,000 metres above sea level. The analysis was carried out for January 2018 because of the high amount of snow that fell in a short period, making the levels of fresh snow accumulation greater than average.

Today's pupils will live in cities that are organized in a fundamentally different way compared to present urban spaces. They will live in smart cities. Three developments have facilitated the spread of the smart city: more efficiently. Ideally, citizens have more influence through e-participation in governmental decisions (Mandl & Zimmermann-Janschitz, 2014, p. 616).

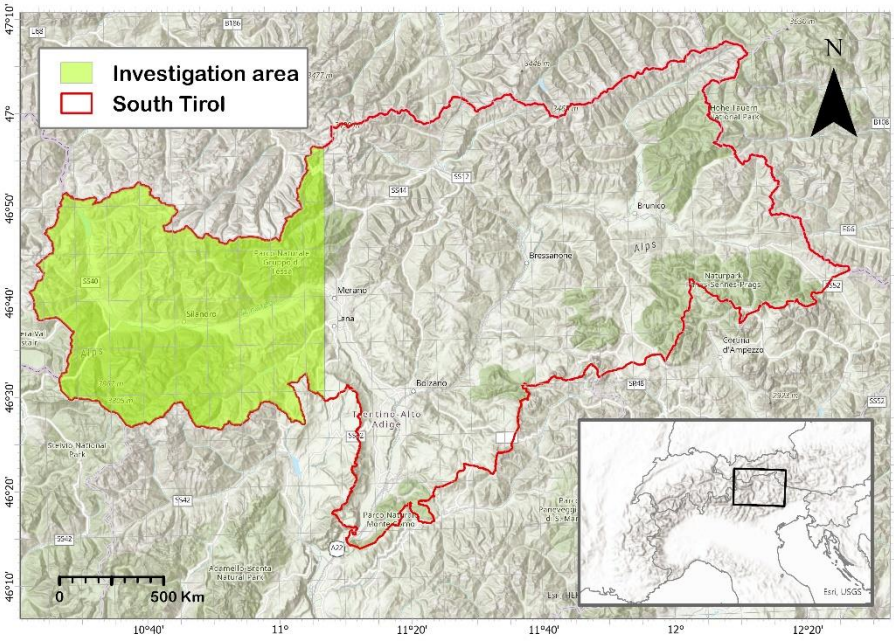

Figure 1: The study area, in the western part of the southern Tyrol, north-eastern Italian Alps.

For the investigation period, a baseline image (no avalanche) from 11/01/2018 was selected and compared to a post-event image from 23/01/2018. In the later image, pixels that show an increase in backscatter are likely to indicate a zone of avalanche debris, since scattering increases with surface roughness. No relevant avalanche activity could be expected on the 11/01/2018 based on meteorological data and precipitation records. Furthermore, all reported avalanches were recorded after the 15/01/2018.

We used freely available Sentinel-1 SAR data from European Space Agency Copernicus, with Ground Range Detected Interferometric Wide swathe, and images in vertical-vertical (VV) and vertical-horizontal (VH) polarizations. We used constellations from Sentinel-1 SAR A and B to reduce the temporal baseline to six days; the ascending flight direction (south–north) was chosen for analysis, since complete coverage of the investigation area is guaranteed by always using the same orbital path and frame for Sentinel-1 satellites A and B. The minimum mapping unit that Sentinel-1 SAR data make possible is directly connected to the available spatial resolution of 20 metres. Avalanche debris less than 20 metres wide cannot be reliably detected.

The pre-processing of the SAR data included orbit file correction, calibration, terrain correction, and transforming pixel values into decibels using SNAP software. To perform change detection, Sentinel-1 SAR image pairs of a baseline image and a post-event image twelve days later (where avalanches could potentially be present) were created. A median filter was applied to reduce noise but preserve edges (Leinss et al., 2020). Change detection was done for each polarization band (i.e., VV and VH) separately, by subtracting the baseline image from the post-event image. In the next step, iterative self-organizing (ISO) and K-means data analysis techniques were applied to produce classes consisting of pixel clusters with similar mean backscatter values. This task was performed using the semi-automatic classification plugin in QGIS (Congedo, 2023). To improve the results, a classification sieve was applied, using a threshold size of one pixel (corresponding to 40 square metres); avalanches smaller than this are not considered dangerous for people (Eckerstorfer et al., 2019). This method removes small clusters from the classification by replacing isolated pixels with the values of the largest neighbour patch. The resulting classes were analysed, and a binary class of avalanche and non-avalanche pixels areas was created.

In the next step, classification results were refined by minimizing the errors due to (a) topography, and (b) SAR side-looking geometry. For the former, information was derived from a very-high-resolution digital elevation model (DEM) showing slope and run-out zones (where debris is likely to be found). To minimize geometry-related error, information for shadow and layover was used (i.e. where the SAR signal could not reach the earth's surface). Some slopes are too steep for avalanche debris to accumulate. Consequently, except for very small avalanches, the limit can be set at 35° (Bühler et al., 2009). Slopes steeper than that were masked out. An avalanche run-out zone can be inferred using a dedicated toolbox, 'Terrain Analysis Using Digital Elevation Models' (TauDEM) (Tarboton, 2023) and the potential release area (PRA). The TauDEM toolbox comprises tools for extracting and analysing hydrological information from topography; it also has a specialized function that evaluates potential avalanche run-out zones. PRA is calculated using a Python script (Bertschinger, 2022), based on Bühler et al. (2018), which uses parameters such as terrain slope and curvature. The avalanche run-out zone is therefore the target area for the semi-automatic avalanche debris detection. Finally, shadow and layover areas in the satellite image, where the SAR signal

could not reach the earth's surface due to the angle of the radar beam in relation to the mountainous terrain, were masked out, since they contain no useful data. The methodology workflow is summarized in Figure 2.

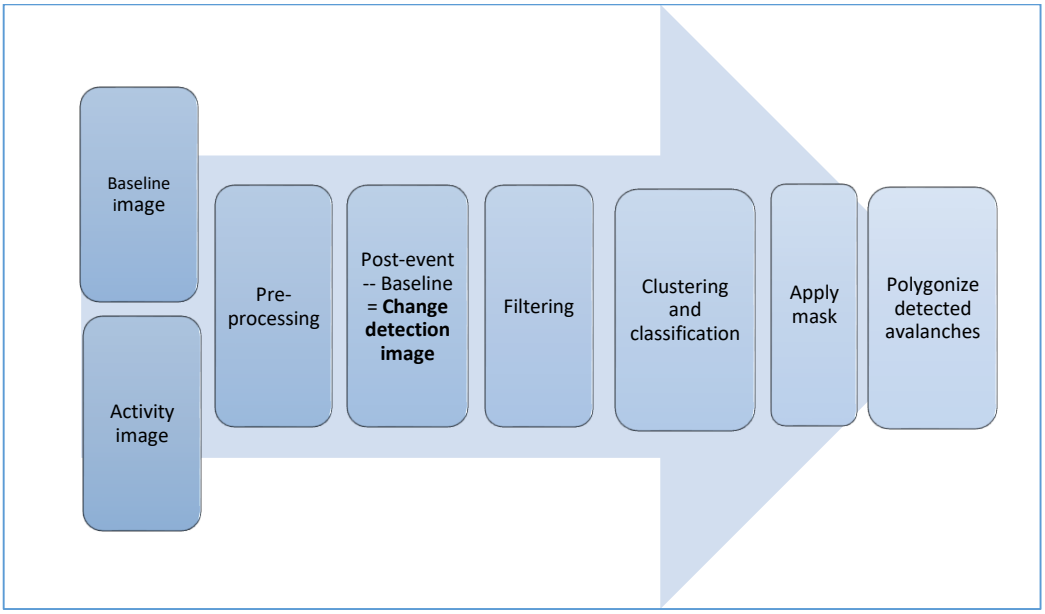

Figure 2: Overall methodology applied to Sentiel-1 SAR images to obtain avalanche debris polygons

3 Results

After a significant amount of snow fell within a few days, 23 avalanches were reported within the investigation area on 22 January 2018. However, as only events causing damage or casualties are reported, it is possible that many more avalanches occurred during those few days.

The results showed that 20% more avalanches could be correctly identified using the VH cross-polarization band compared to the VV co-polarization band. These results are in line with the literature (e.g. Wesselink et al. (2017)), which states that VH polarization is generally more susceptible than VV polarization to surface scattering produced by rough avalanche debris.

A visual inspection of the results showed that a large number of avalanches were located at lower altitudes, beneath densely forested areas. These lower altitudes often coincide with cultivated meadows that are known to be sensitive to changes in backscatter values when covered by snow (Eckerstorfer et al., 2019), a sensitivity which could lead to false positives in the detection of avalanches at these lower levels. The results were therefore refined by masking out the avalanches below the forests (the forests in this region grow at approximately 2,000m

upwards). The knock-on effect of this measure is that avalanches occurring below 2,000m will be missed.

Of the avalanches reported, 30% were correctly detected, 13% were missed, and 21% lay within the masked-out areas. 34% of avalanches were partially detected. A partial detection happens when small, discontinuous patches of avalanche debris are identified within the confines of a reported avalanche, without them covering the whole expected run-out zone.

An example of a correctly identified avalanche can be seen in Figures 3 and 4.

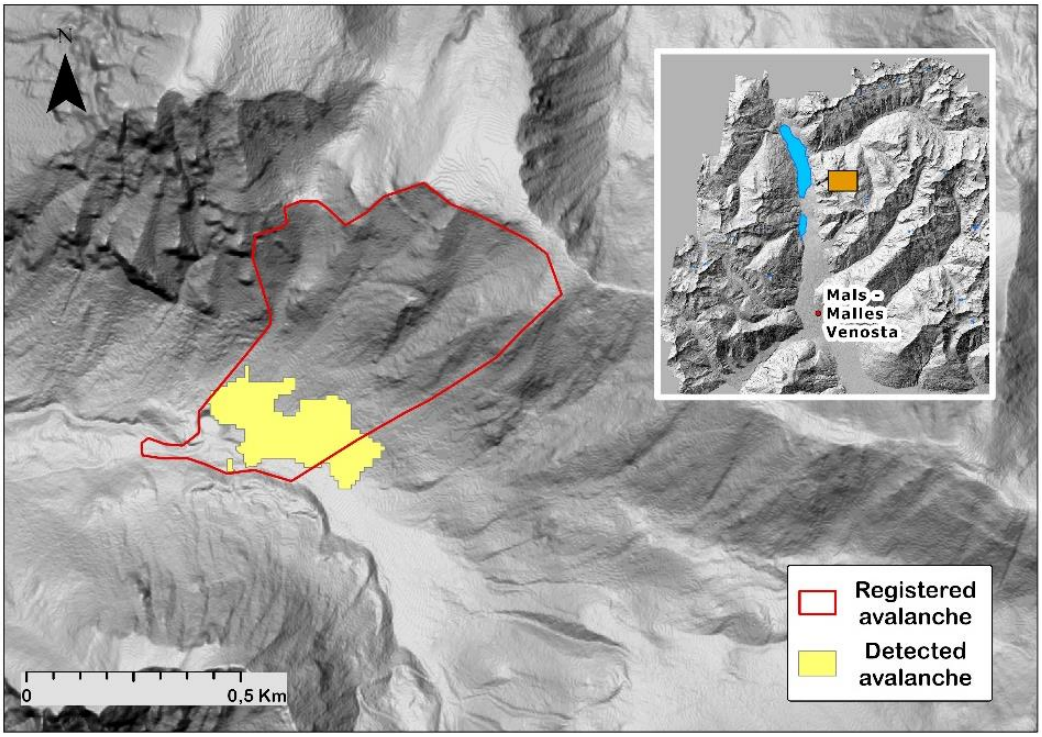

Figure 3: Avalanche debris identified by the classification process. Hillshade background derived from a 5-metre DEM made available by the local authorities (Suedtiroler Buergernetz, 2023).

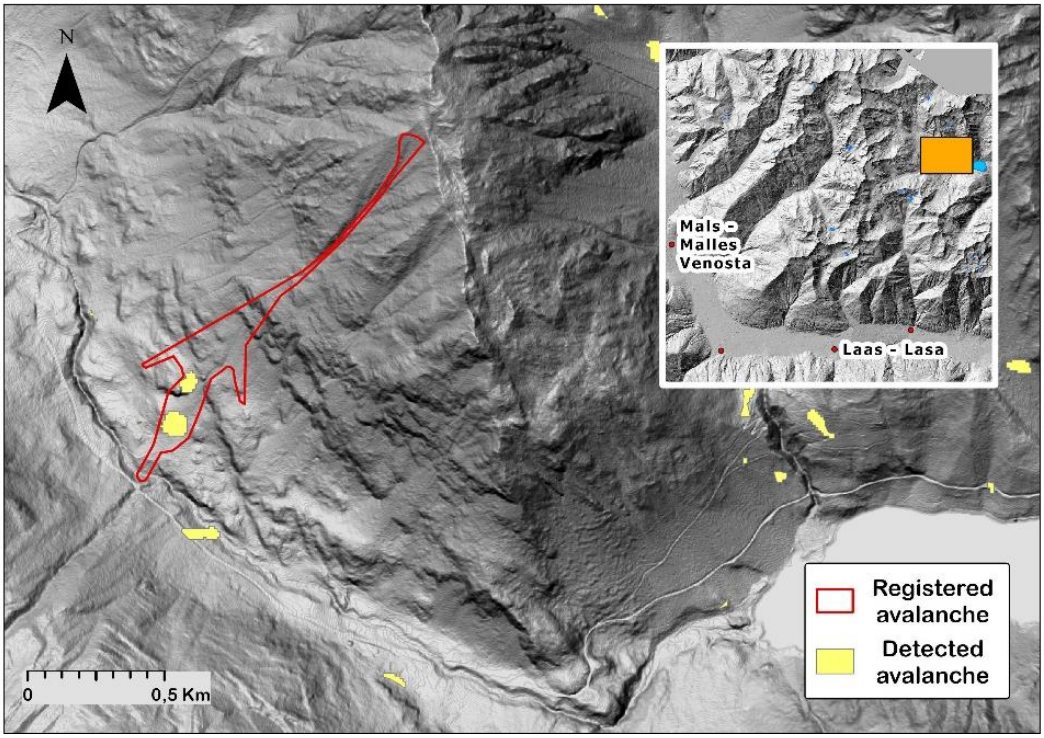

Figure 4: Avalanche debris identified by the classification process. Hillshade background derived from a 5-metre DEM made available by the local authorities (Suedtiroler Buergernetz, 2023).

Figure 5 shows how avalanche debris identification is carried out using SAR data. In this case, a composite colour image has been used to show increase in backscatter values in green, and decrease in backscatter values in purple. In the manual avalanche detection process, referred to as RGB differentiation, a composite image is constructed of the red and blue channels (containing the reference image), and the green channel (which contains the avalanche activity image). Pixels that show increased backscatter values between the baseline image and post-event image appear green; pixels with decreased backscatter appear purple; pixels that witnessed no change appear grey. The red polygon represents a reported avalanche and is used as a reference to show where increased values of backscatter are to be expected.

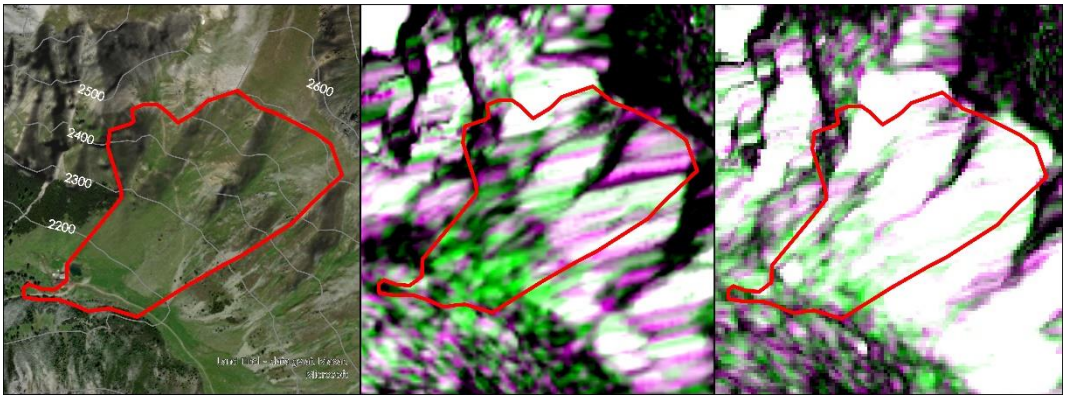

Figure 5: Comparison of a reported avalanche (left) with two SAR images, in false colour composite. Green shows an increase in backscatter values, purple a decrease in backscatter values. Centre: VV polarization; right: VH polarization.

4 Discussion and Conclusions

The avalanche detection model is able to locate only the run-out zone of an avalanche, i.e. the lower third, where snow stops and piles up (Figure 3). The model proves to be reliable, since 79% of the officially reported avalanches were detected from SAR images. This is in line with Hafner et al. (2021) who, using the same methodology, reported that 50%–74% of avalanches were correctly identified. Missed detection of avalanche debris, amounting to 21% of the total reported avalanches, could be due to avalanche debris shape and size, or SAR imagery limitations such as shadow and overlay. Avalanche debris that is sub-pixel level in size cannot be detected reliably (Eckerstorfer et al., 2019). Therefore, avalanche debris less than 40m wide was eliminated to reduce the false alarm rate. This may, however, have led to missed avalanche detections. Higher spatial resolution SAR data needs to be investigated to address this issue. Furthermore, avalanche debris that is elongated in shape cannot be detected, even if its size is considerable.

Of the avalanches identified, 46% were fully detected, while 54% were partially detected. As 21% of reported avalanches lay within the masked-out areas, only 13% of the total were missed entirely. Classifications performed using the ISO and K-means methods produced very similar results: K-means clustering identified 2% more pixels belonging to the class 'avalanche'; however, the final number of avalanches identified was the same whether ISO or K-means was used.

The analysis revealed some limitations in avalanche detection, as described in more detail below.

False positives: One major problem are avalanches spotted on agricultural land: as the method is sensitive to surface roughness change, it can lead to false positives because it is not possible to determine whether the ground is covered with dry snow or no snow based on C-band SAR data (Eckerstorfer et al., 2019). Another cause for false detection is the transformation of snow from wet to dry due to meteorological conditions. Since the snow-

pack tends to become consolidated in dry conditions, such days could be excluded from analysis as avalanches can generally be ruled out in these conditions (Tompkin & Leinss, 2021).

Verification: Officially reported and mapped avalanches are too few in number to produce a reliable verification process. Field validation would be needed to confirm the results of the model, but the remoteness and inaccessibility of the areas analysed are major obstacles. High-resolution (less than 10m) space-borne optical images could be used to confirm detected events. Data from the Pléiades-HR satellite launched by the French National Centre for Space Studies with 0.5m resolution could be used for this purpose.

The model tested in this research returns satisfactory results and could be applied regionally for the semi-automatic detection of avalanches. However, further improvements are needed to assess its reliability. For example, local resolution weighting could be applied on backscatter images to increase avalanche brightness, and to improve image coverage and resolution before classification (Tompkin & Leinss, 2021). Another approach that promises improved performance involves the application of K-means classification to SAR images before change detection is performed (Vickers et al., 2017). Lastly, the reliability of the proposed workflow should be assessed by applying it on larger spatial and temporal scales, e.g. for the whole region of the southern Tyrol during an entire winter season.

References

Bertschinger, T. (2022). *Automated mapping of potential snow avalanche release areas (PRAs)*. https://github.com/unibe-geodata-modelling/2018-snow-avalanches-sources

Bianchi, F.M., Grahn, J., Eckerstorfer, M., Malnes, E. and Vickers, H. (2021). Snow Avalanche Segmentation in SAR Images with Fully Convolutional Neural Networks. *IEEE Journal of Selected Topics in Applied Earth Observations and Remote Sensing, 14*, pp. 75–82. Available at: https://doi.org/10.1109/JSTARS.2020.3036914.

Bühler, Y., Hüni, A., Christen, M., Meister, R., & Kellenberger, T. (2009). Automated detection and mapping of avalanche deposits using airborne optical remote sensing data. *Cold Regions Science and Technology*, *57*(2–3), 99–106. https://doi.org/10.1016/j.coldregions.2009.02.007

Bühler, Y., von Rickenbach, D., Stoffel, A., Margreth, S., Stoffel, L., & Christen, M. (2018). Automated snow avalanche release area delineation – validation of existing algorithms and proposition of a new object-based approach for large-scale hazard indication mapping. *Natural Hazards and Earth System Sciences*, *18*(12), 3235–3251. https://doi.org/10.5194/nhess-18-3235-2018

Congedo, L. (2023). *Semi-Automatic Classification Plugin*. https://plugins.qgis.org/plugins/SemiAutomaticClassificationPlugin/

EAWS. (2023). *European Avalanche Warning Services. Fatalities*. https://www.avalanches.org/fatalities/

Eckerstorfer, M., Vickers, H., Malnes, E., & Grahn, J. (2019). Near-Real Time Automatic Snow Avalanche Activity Monitoring System Using Sentinel-1 SAR Data in Norway. *Remote Sensing*, *11*(23), 2863. https://doi.org/10.3390/rs11232863

Hafner, E. D., Barton, P., Daudt, R. C., Wegner, J. D., Schindler, K., & Bühler, Y. (2022). Automated avalanche mapping from SPOT 6/7 satellite imagery with deep learning: Results, evaluation, potential and limitations. *The Cryosphere*, *16*(9), 3517–3530. https://doi.org/10.5194/tc-16-3517-2022

Hafner, E. D., Techel, F., Leinss, S., & Bühler, Y. (2021). Mapping avalanches with satellites – evaluation of performance and completeness. *The Cryosphere*, *15*(2), 983–1004. https://doi.org/10.5194/tc-15-983-2021

Kumar, S., Narayan, A., Mehta, D., & Snehmani. (2022). Snow cover characterization using C-band polarimetric SAR in parts of the Himalaya. *Advances in Space Research*, *70*(12), 3959–3974. https://doi.org/10.1016/j.asr.2022.10.012

Leinss, S., Wicki, R., Holenstein, S., Baffelli, S., & Bühler, Y. (2020). Snow avalanche detection and mapping in multitemporal and multiorbital radar images from TerraSAR-X and Sentinel-1. *Natural Hazards and Earth System Sciences*, *20*(6), 1783–1803. https://doi.org/10.5194/nhess-20-1783-2020

McClung, D. M. (2002). The Elements of Applied Avalanche Forecasting, Part II: The Physical Issues and the Rules of Applied Avalanche Forecasting. *Natural Hazards*, *26*(2), 131–146.
https://doi.org/10.1023/A:1015604600361

Muller, K., Eckerstorfer, M., Grahn, J., Malnes, E., Engeset, R., Humstad, T., & Widforss, A. (2021). Norway's Operational Avalanche Activity Monitoring System Using Sentinel-1. *2021 IEEE International Geoscience and Remote Sensing Symposium IGARSS*, 236–238. https://doi.org/10.1109/IGARSS47720.2021.9553152

Sinha (2019). Can Avalanche Deposits be Effectively Detected by Deep Learning on Sentinel-1 Satellite SAR Images?

Suedtiroler Buergernetz. (2023). *GeoKatalog*. http://geokatalog.buergernetz.bz.it/geokatalog/#!

Tarboton, D. (2023). *Terrain Analysis Using Digital Elevation Models (TauDEM)*. https://hydrology.usu.edu/taudem/taudem5/

Tompkin, C., & Leinss, S. (2021). Backscatter Characteristics of Snow Avalanches for Mapping With Local Resolution Weighting. *IEEE Journal of Selected Topics in Applied Earth Observations and Remote Sensing*, *14*, 4452–4464. https://doi.org/10.1109/JSTARS.2021.3074418

Vickers, H., Eckerstorfer, M., Malnes, E., & Doulgeris, A. (2017). Synthetic Aperture Radar (SAR) Monitoring of Avalanche Activity: An Automated Detection Scheme. In P. Sharma & F. M. Bianchi (Eds.), *Image Analysis* (Vol. 10270, pp. 136–46). Springer International Publishing. https://doi.org/10.1007/978-3-319-59129-2_12

Wesselink, D.S., Malnes, E., Eckerstorfer, M. and Lindenbergh, R.C. (2017). Automatic detection of snow avalanche debris in central Svalbard using C-band SAR data. *Polar Research*, 36(1), p. 1333236. Available at: https://doi.org/10.1080/17518369.2017.1333236.

Wiesmann, A., Wegmuller, U., Honikel, M., Strozzi, T., & Werner, C. L. (2001). Potential and methodology of satellite based SAR for hazard mapping. *IGARSS 2001. Scanning the Present and Resolving the Future. Proceedings. IEEE 2001 International Geoscience and Remote Sensing Symposium* (Cat. No.01CH37217), *7*, 3262–64. https://doi.org/10.1109/IGARSS.2001.978322

Yang, J., Li, C., Li, L., Ding, J., Zhang, R., Han, T., & Liu, Y. (2020). Automatic Detection of Regional Snow Avalanches with Scattering and Interference of C-band SAR Data. *Remote Sensing*, *12*(17), 2781. https://doi.org/10.3390/rs12172781